Studies on the Thermal Re-ignition in SF_6 High-Voltage Circuit-Breakers by means of Coupled Simulation

Reichert F. [1], Petchanka A. [1], Freton P. [2], Gonzalez J. J. [2]

[1]*Siemens AG, EM HP CB R&D E, Nonnendammallee 104, 13629 Berlin, Germany*
frank.reichert@siemens.com
[2]*Université de Toulouse, LAPLACE, 118 route de Narbonne, CNRS-UPS-INP,*
F-31062 Toulouse, France

The paper presents a modelling approach to study the switching capacity of SF_6 high-voltage circuit breakers with respect to the thermal re-ignition. This approach is based on the coupling of a model for the thermal re-ignition and a model describing the transient response of an external circuit. It is pointed out that the switching capacity can be evaluated taking into account the simulated trends for the transient recovery voltage similar to the approach in real tests. The different behaviour of the regarded SF_6 self-blast circuit-breaker at different arcing times is highlighted using simulation results for pressure, temperature and electrical conductivity.

Keywords: high-voltage circuit-breaker, CFD, switching arc, thermal re-ignition

1 INTRODUCTION

The switching capacity of SF_6 high-voltage circuit-breakers depends, as one of many effects, on the regarded arcing time. This is clarified by the test protocol of a short-line fault (SLF) interruption acc. to Fig. 1. At a SLF interruption the switching gap fails by thermal re-ignition due to the very fast rise of the transient recovery voltage (TRV).

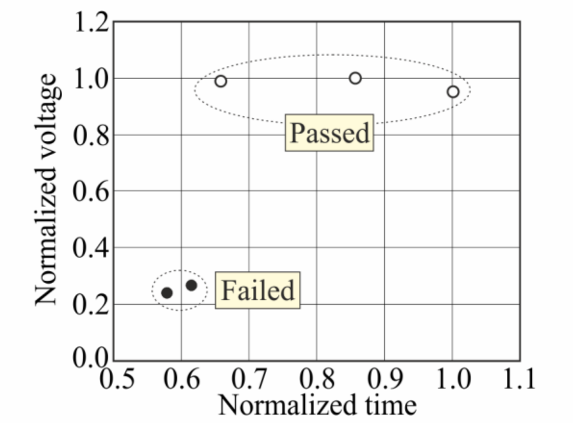

Fig. 1: Test protocol of a SLF interruption

The time line of Fig. 1 is normalized by the maximum arcing time and the voltage values by the maximum peak value of the TRV in the test series. The white coloured circles in Fig. 1 characterise successful switching-off processes (“Passed”) with high peak values of the TRV similar to unaffected trend and the black coloured circles characterise non-successful switching-off processes (“Failed”) with very low peak values of the TRV. In order to highlight the reasons for the different behaviour depending on the arcing time with respect to the thermal re-ignition in more detail a simulation model was developed and applied in the simulation of the switching-off process in a real SF_6 self-blast circuit-breaker. The mentioned simulation model couples a sub model for the thermal re-ignition and a sub model for the external circuit in the post arc simulation. For the evaluation of the SLF interruption capability the simulated trend of the TRV is used. Thus it is possible to visualize the simulated switching capacity of the regarded circuit breaker in a diagram similar to the test protocol acc. to Fig. 1 which is very useful in the development process of high-voltage circuit-breakers. This approach is different to approaches from the literature e.g. [1, 2]. For instance in [1] the trend of the post arc current calculated with different constant rises of recovery voltage is taken to evaluate the SLF interruption capability. In [2] a SLF interruption performance index is used which combines the pressure in the heating volume and the density above the arc zone.

2 MODELLING

2.1 SIMULATION MODEL

The numerical simulation and thus the description of the fluid mechanical processes in the interrupter unit (IU) of SF_6 self-blast circuit-breakers during the switching-off process is carried out using a modular simulation model which is based on the CFD program ANSYS/FLUENT. Fig. 2 shows the set-up of the simulation model. The switching mechanics are considered by dynamic models for the drive and the valve operation taking into account the pressure force calculated in the CFD arc simulation. Thus the interaction between the switching arc and the switching mechanics can be simulated. The switching arc is reflected by a real gas model for the mixture of SF_6 and C_2F_4, a dynamic arc model taking into consideration Ohmic heating, radiation and nozzle ablation and a model for the evaluation of the switching capacity after current zero.

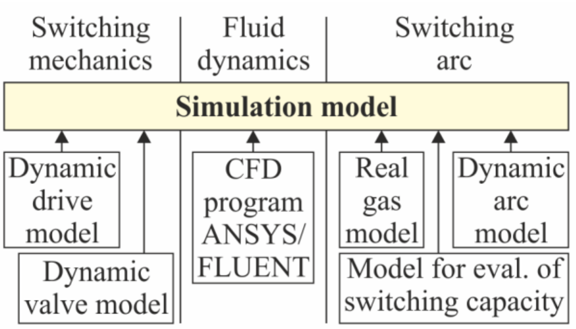

Fig. 2: Set-up of simulation model

The Ohmic heating term is evaluated using a predefined current density profile. The radiative transfer is simulated by a mixed formulation based on the combination of the P1 and DO model acc. to [3]. The model for the consideration of nozzle ablation takes into account pre-heating of PTFE nozzle walls, pyrolysis and evaporation [4]. Turbulent effects are considered by the realizable k-ε model. The modelling approach to study the switching capacity of SF_6 high-voltage circuit-breakers with respect to the thermal re-ignition is highlighted in the next section.

The studies have been carried out on the interrupter unit geometry of a real SF_6 self-blast circuit-breaker. In Fig. 3 a part of the respective solution domain is shown.

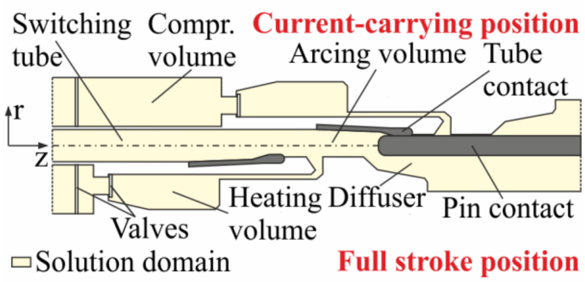

Fig. 3: Part of the solution domain

The variation of solution domain and discretisation during the simulation is controlled by the dynamic models for the drive and valve operation.

2.2 MODELLING IN THE POST ARC PHASE

As already mentioned, in the post arc phase a model for the thermal re-ignition is coupled with a model describing the transient response of the external circuit, see Fig. 4.

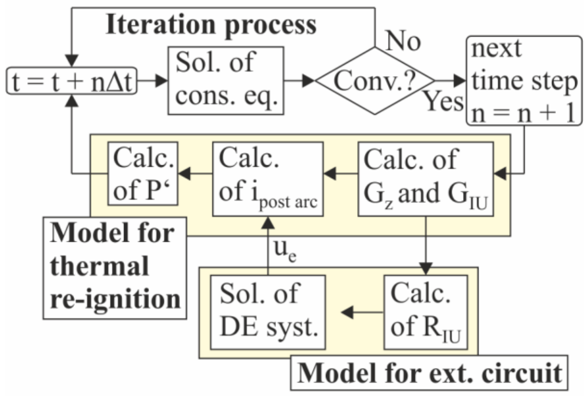

Fig. 4: Flow chart for the simulation after current zero

After current zero the contact gap is stressed by the TRV named u_e in Fig. 4. This voltage causes a post arc current through the remaining arc channel which heats the leftover plasma and leads possibly to the thermal re-ignition of the contact gap. To describe this behaviour the iteration process in each time step of the flow simulation after current zero is carried out considering a special source term in the energy equation P'. The model for the thermal re-ignition delivers the post arc current $i_{post\ arc}$ and hence this source term, see Fig. 4. The calculation of P' is realized acc. to [5] by the following equation

$$P' = \sigma\left(\frac{i_{post\ arc}}{G_z}\right)^2 . \tag{1}$$

In eq. (1) σ is the electrical conductivity and G_z corresponds to the conductance of a radial orientated layer along the axis of the remaining arc channel. In the model for the external circuit the value of the contact gap resistance R_{IU} is calculated firstly by $R_{IU}=1/G_{IU}$ where G_{IU} is the entire contact gap conductance, see Fig. 4. This resistance is considered in the electrical network for the regarded external circuit. As an example for the external circuit Fig. 5 shows the circuit diagram for a basic high-voltage circuit which can be used to test the SLF interruption capability.

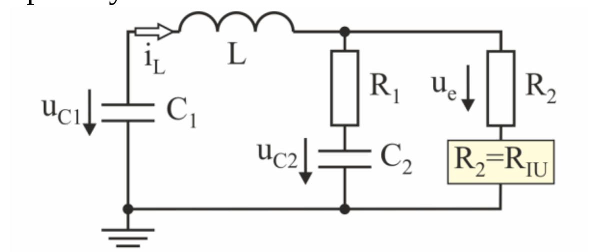

Fig. 5: Circuit diagram of high-voltage circuit

The mathematical model for the description of the transient process in the high-voltage circuit is given by eq. (2)

$$\frac{d}{dt}\begin{pmatrix} u_{C_1} \\ i_L \\ u_{C_2} \end{pmatrix} = \begin{pmatrix} 0 & -\frac{1}{C_1} & 0 \\ \frac{1}{L} & -\frac{R_1 R_2}{(R_1+R_2)L} & -\frac{R_2}{(R_1+R_2)L} \\ 0 & \frac{R_2}{(R_1+R_2)C_2} & -\frac{1}{(R_1+R_2)C_2} \end{pmatrix}\begin{pmatrix} u_{C_1} \\ i_L \\ u_{C_2} \end{pmatrix}. \quad (2)$$

After the solution of the equation system acc. to eq. (2) the TRV u_e can be calculated by

$$u_e = R_2\left(i_L \frac{R_1}{R_1+R_2} + u_{C_2}\frac{1}{R_1+R_2} \right), \quad (3)$$

and the post arc current by

$$i_{post\ arc} = \frac{u_e}{R_{IU}}. \quad (4)$$

Using this modelling approach the interaction between the post arc and the transient response in the external circuit can be simulated.

3 SIMULATION RESULTS

The switching-off process in the regarded real SF_6 self-blast circuit-breaker was simulated for three different arcing times: short arcing time ($t_{arc,1}$), medium arcing time ($t_{arc,2}$) and long arcing time ($t_{arc,3}$). Fig. 6 shows the respective current trends which were multiplied for the simulation by a current rms value of $I_{rms} = 36$ kA. Additionally in Fig. 6 the measured and simulated peak values of the TRV are depicted in comparison. As it can be seen from Fig. 6 the simulation model predicts the switching capacity very similar to the test series. The time axis and the voltage values in Fig. 6 are normalized corresponding to Fig. 1. As the regarded SF_6 self-blast circuit-breaker shows in the simulation for $t_{arc,2}$ and $t_{arc,3}$ nearly the same behaviour the following evaluation of the simulation results is only done using the simulation results at $t_{arc,1}$ and $t_{arc,2}$. It shows that the conditions with respect to a successful switching-off process are clearly worse at $t_{arc,1}$ than at $t_{arc,2}$. This is obviously by the comparison acc. to Fig. 6.

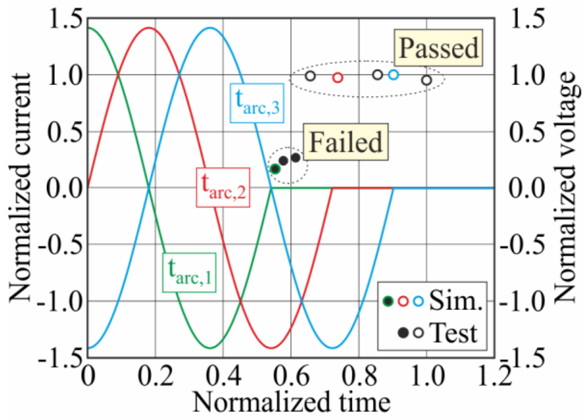

Fig. 6: Current trends and peak values of TRV

The pressure build-up in the heating volume during the high-current phase is clearly lower at $t_{arc,1}$ which leads to a reduced gas flow from the heating volume to the arcing volume at current zero. Thus there are lower values of pressure and higher values of temperature in the arcing volume at $t_{arc,1}$. In that case the pressure in the stagnation point reaches only about 35% of the pressure in the case of the medium arcing time. Concerning the temperature the differences are less. According to [6], the higher the pressure and the lower the temperature, the lower is the electrical conductivity.

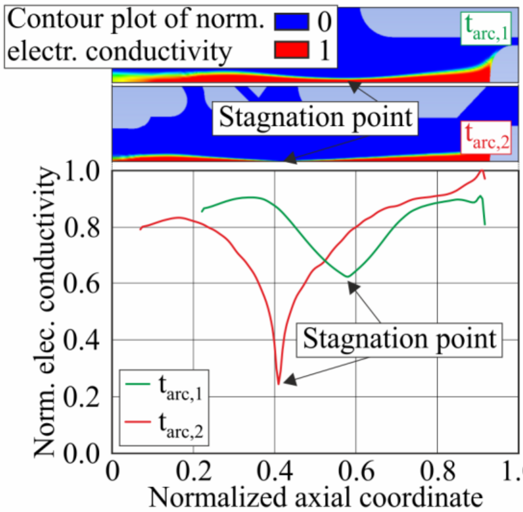

Fig. 7: Axial distribution of electrical conductivity at current zero

Hence the values for the electrical conductivity in the arcing volume are clearly higher at $t_{arc,1}$, see Fig. 7. Additionally the diameter of the remaining arc channel, especially in the stagnation point, is greater at $t_{arc,1}$ than at $t_{arc,2}$., see the contour plot of the electrical conductivity in Fig. 7.

The higher values of the electrical conductivity and the greater diameter of the remaining arc channel lead to a lower resistance of the contact gap in and just after the current zero when the contact gap is stressed by the TRV. This is obviously by the comparison acc. to Fig. 8.

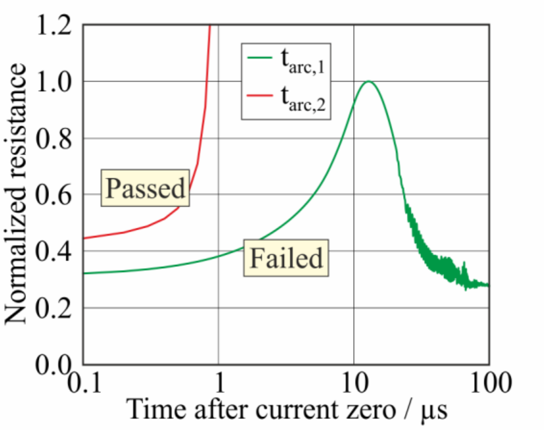

Fig. 8: Temporal evolution of contact gap resistance after current zero

In dependence on the contact gap resistance the TRV forces the post arc current through the leftover plasma. At $t_{arc,2}$ this post arc current is so small that the resulting heating cannot prevent the further cooling of the leftover plasma. By this reason the contact gap resistance increases at about 1 µs after current zero very strongly and the TRV oscillates over the contact gap similar to the unaffected trend characterising a successful switching-off process ("Passed"), see Fig 9.

At $t_{arc,1}$ a greater post arc current heats the leftover plasma and the contact gap resistance increases slower. After about 20 µs the heating overcomes the cooling of the leftover plasma resulting in a strong drop of the contact gap resistance, see Fig. 8. Acc. to Fig. 9 the oscillating TRV follows the trend of the contact gap resistance and reaches less than 20% of the maximum value from the trend in case of the medium arcing time $t_{arc,2}$.

Such a trend for the transient recovery voltage characterises a non-successful switching-off process ("Failed").

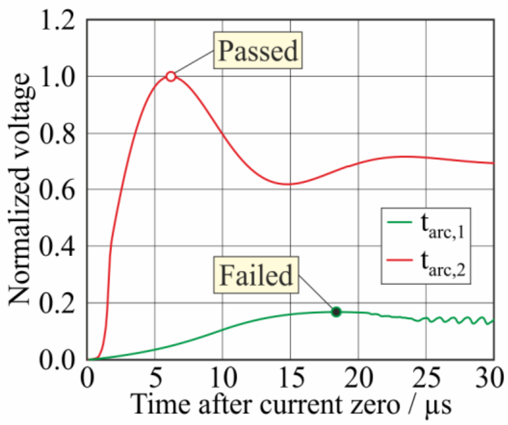

Fig. 9: Simulated trends for the TRV

4 CONCLUSION

For the post arc simulation the presented simulation model enables the consideration of the interaction between the post arc and the transient response in the external circuit. It delivers the trend of the TRV which can be used to evaluate the SLF interruption capability of the regarded SF_6 high-voltage circuit-breaker. It has been found out that the pressure and the temperature in the arcing volume and hence the electrical conductance of the remaining arc channel differ very strongly at current zero depending on the arcing time. In case of too high values for the electrical conductivity and the diameter of the remaining arc channel especially in the stagnation point the switching-off process fails.

REFERENCES

[1] Lee J C et al., In: 20th Symp. on Physics of Switching Arc, Czech Republic (2013) 232-235.

[2] Kim H K et al., J. Electr. Eng. Technol. 8 (2013) 742-746.

[3] Reichert F et al., J. Phys. D: Appl. Phys. 45 (2012) 375201.

[4] Gonzalez J J et al., IEEE Trans. on Plasma Science submitted.

[5] Gonzalez J J et al., J. Phys. D: Appl. Phys. 33 (2000) 2759–2768.

[6] Chevry B et al., J. Phys. D: Appl. Phys. 27 (1994) 1193–1208.